

Internal energy of sputtered metal clusters

A. Wucher

Fachbereich Physik, Universität Kaiserslautern, D-67663 Kaiserslautern, Federal Republic of Germany

(Received 9 July 1993)

The internal excitation of silver clusters sputtered from a polycrystalline silver surface by Ar^+ ions of 5 keV was investigated by laser postionization of the ejected neutral species and time-of-flight mass spectrometry. For sputtered dimers, resonant two-photon ionization spectroscopy was employed using either a one- or a two-color scheme. From the resulting spectra, vibrational and rotational population temperatures around 2700 and 6700 K are determined which agree well with corresponding predictions obtained from molecular-dynamics simulations of the molecule sputtering process. For larger clusters, single-photon ionization by a fixed frequency laser was used for cluster detection and the spectra obtained with different laser wavelengths were compared. The results show that around 50% of the sputtered Ag_6 clusters are formed with internal energies in excess of 0.75 eV.

I. INTRODUCTION

It is well known that the flux of particles sputtered from a solid surface by energetic ions may contain agglomerates of several atoms. The fundamental processes leading to the formation of these sputtered clusters, however, are still not completely understood. In the so-called linear cascade regime of the sputtering process,¹ the atomic ejection following a primary ion impact event is caused by elastic collisions between the atoms in a sub-surface region of the bombarded solid, and hence the molecule formation will be also collision dominated. Various theoretical model descriptions of cluster sputtering have appeared in the literature ranging from conceptually simple statistical considerations²⁻⁸ to fairly sophisticated molecular-dynamics computer simulations.⁹⁻²⁰ Besides the yields (i.e., the average number of clusters ejected per impinging primary ion), most of these models also allow predictions of the translational and—in some cases—the internal energy distribution of sputtered clusters. It is particularly the latter quantity which we focus on in the present paper, since it has been suggested that the internal energy distribution may serve to distinguish between the different molecule formation mechanisms.

A general prediction of the theoretical models mentioned above is that sputtered clusters are *hot*, i.e., on the average exhibit a high degree of internal (vibrational and rotational) excitation. This prediction, which is intuitively expected due to the collision processes generating the cluster, still lacks a sound experimental verification. The only experimental data on internal energies of sputtered clusters published to date were measured on diatomic molecules. In particular, experiments were performed for (i) a number of diatomics emitted from silicon containing various impurities²¹ and from several elements bombarded with N_2^+ ions,^{22,23} (ii) S_2 dimers sputtered from elementary sulphur and CS_2 targets^{24,25} and (iii) a few alkali dimers²⁶ (Na_2 , K_2 , and Cs_2). In the first case, extremely broad rotational population distributions with pronounced non-Boltzmann character were reported. In the second case, quasithermal vibrational population distri-

butions were determined showing a vibrational temperature of 1500 K, whereas the rotational population was found to be strongly nonthermal. In the third case, thermal distributions were assumed and an internal population temperature of 1000 K was deduced. In the present paper, we investigate the internal excitation of sputtered *silver* clusters, since the ion bombardment induced removal of particles from a high-melting metallic sample represents an almost ideal example of collisional sputtering, in particular if rare-gas ions of energies in the keV range are used²⁷ to bombard the solid. In a first part of this work, we try to determine the internal temperature of sputtered silver *dimers* by laser spectrometrical methods. For clusters containing three or more atoms, no direct data on internal energy distributions exist in the literature. The only experimental approach to the subject which has been successful up to now is the analysis of unimolecular decomposition rates of sputtered cluster ions.²⁸⁻³³ These results clearly demonstrate the existence of hot clusters within the sputtered flux. They do not, however, allow a quantitative determination of the fraction of excited species among the total flux of sputtered clusters and are therefore difficult to interpret in terms of average internal energies. In a second part of this work, we present the first direct experimental hint on the average amount of internal energy stored in sputtered metal clusters larger than dimers.

II. EXPERIMENT

The experiments were performed using a reflectron time-of-flight mass spectrometer sketched in Fig. 1 which was mounted in an ultrahigh vacuum chamber (base pressure 1×10^{-9} mbar). The setup has been described in great detail elsewhere³⁴ and, hence, only a brief summary of the operating parameters will be given here. A polycrystalline silver sample was bombarded under 45° with a pulsed 5-keV Ar^+ ion beam of $5 \mu\text{A}$. During the ion pulse, the sample potential was kept at -300 V with respect to ground in order to keep positive secondary ions produced during this time from leaving the surface.

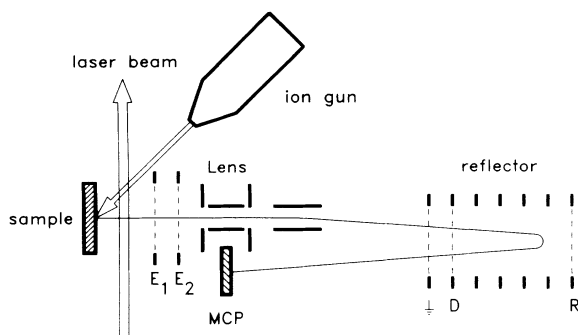


FIG. 1. Schematic setup for Laser ionization and time-of-flight mass spectrometry of sputtered clusters.

At 200 ns after the end of the primary pulse, a pulsed laser was fired, whose beam of approximately 1-mm diameter was directed parallel to the sample surface at a distance of approximately 1 mm, and sputtered neutral clusters generated during the primary ion pulse were ionized by different ionization schemes as described below. The photoionized clusters were extracted towards the mass spectrometer by an accelerating field established by switching the sample potential to +1500 V shortly (~ 20 ns) after the laser was fired. With both extraction grids (E_1 , E_2) as well as the field-free drift space being at ground potential, the ions enter the mass spectrometer with a kinetic energy of around 1300 eV, are reflected by an electrostatic mirror tuned for optimum energy refocusing conditions [grids (D) and (R) operated at potentials of +440 V and +1400 V with respect to ground] and are then detected by a Chevron stack of microchannel plates. The mass resolution achieved under these conditions (typically $m/\Delta m \approx 500$ at $m = 216$ amu) was high enough to completely resolve the different isotopomers of the silver dimer. The optical setup used throughout the present experiments is displayed in Fig. 2. Basically, two different photoionization schemes were employed to detect the sputtered neutral dimers on one hand and larger clusters on the other hand which in the following will be described separately.

For *dimers*, a resonant two-photon ionization (*R2PI*)

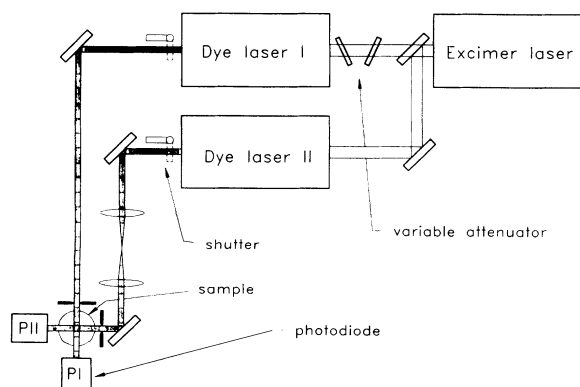


FIG. 2. Optical setup for resonant two-photon ionization and single-photon ionization of sputtered clusters.

process was used involving a resonant transition from the $\text{Ag}_2 X^1\Sigma_g^+$ ground state to the $\text{Ag}_2 C^1\Pi_u$ state and a nonresonant transition from this state to the Ag_2^+ ionization continuum. The resonant excitation was achieved by means of an excimer laser pumped dye laser (Lambda Physik LPD 3002), the output of which was frequency doubled to obtain maximum pulse energies of around 0.2 mJ in the wavelength range between 260 and 280 nm. The ionizing step was performed either by the same laser (one-color scheme) or by a second dye laser (Lambda Physik FL 2000) tuned to a fixed wavelength around 400 nm (two-color scheme). Both laser beams were directed into the vacuum chamber perpendicular to each other, superimposed in the interaction region above the sample surface and shaped such that their spatial full width at half maximum (FWHM) matched the sensitive volume of the mass spectrometer (approximately 1 mm in diameter). The temporal synchronization of the two laser pulses was achieved by pumping both dye lasers with the same excimer laser (Lambda Physik LPX 120i). The pulse energy of the dye lasers was monitored by two fast photodiodes located behind the beam exit windows, which were calibrated by a pyroelectric joulemeter prior to each experiment. During a wavelength scan, the pulse energy of the excitation laser was kept constant within approximately 10% rms by means of a variable dielectric attenuator located in the pump beam path as seen in Fig. 2. For this purpose, the photodiode signal measured by a boxcar integrator was brought back to its initial value by computer controlled tilting of the attenuator every time the wavelength was changed. This was necessary to compensate for the significant variation of the frequency doubled output energy due to (i) the efficiency curve of the dye (Coumarin 307) and (ii) wavelength-dependent changes of the phase matching condition in the frequency doubling crystal. Both lasers were operated without an intracavity etalon at a bandwidth of approximately 0.4 cm^{-1} . The absolute wavelength calibration of the excitation laser was examined by taking *R2PI* spectra of Fe atoms ($4s^2 5D_4 \rightarrow 4s 4p^5 P_J$ transition multiplet) sputtered from the sample holder and was found to be accurate within approximately 10 picometers in the wavelength range studied.

For clusters larger than dimers, *R2PI* spectra become far too complicated for a detailed vibrational and rotational analysis of sputtered molecules. In addition, multiphoton ionization spectra may be largely disturbed by fragmentation processes. Hence, we used a single-photon ionization scheme to detect these species. For this purpose, the excimer laser beam was focused to dimensions of $1.2 \times 2.2 \text{ mm}^2$ (FWHM measured in directions perpendicular and parallel to the sample surface) and directly coupled into the interaction zone above the surface. In order to permit the ionization of silver clusters by single-photon absorption, the excimer laser was now operated with ArF ($\lambda = 193 \text{ nm}$) or F₂ ($\lambda = 157 \text{ nm}$) with maximum pulse energies of around 50 mJ at 193 nm and 1 mJ at 157 nm.

The pulse energies measured for the different lasers were converted into peak power densities by assuming a rectangular temporal pulse profile of 25-ns width. In ad-

dition, the beam cross section area was estimated from the FWHM values of the measured beam profiles. It should be noted that the error introduced by these assumptions may be quite large and, hence, the absolute calibration of the laser power density values given below may be off by as much as a factor of 2.

The ion signals were detected by converting the current produced by the microchannel plate (MCP) into a voltage across a 50- Ω resistor. Time-of-flight (TOF) spectra were recorded either by direct digitization of the resulting voltage pulses, or, at count rates lower than one ion of a certain species per laser shot, by a pulse counting method detecting single ions. In the pulse counting mode, the MCP output was directed to a discriminator forming standard transistor-transistor logic (TTL) pulses of 20-ns width and TOF spectra were acquired by averaging the flight time distribution of pulses over a large number of laser shots. During a wavelength scan, the transient digitizer (LeCroy 9450) was setup as a boxcar integrator and integrated flight time (or mass) peaks were recorded as a function of the excitation laser wavelength. Prior to each experiment, blank spectra were taken with the laser beams blocked which were then subtracted from the measured spectra. In the course of the two-color spectra, each wavelength point was repeated three times and background signals were recorded with either the excitation or ionization laser beam blocked. This way, the spectra could be processed subsequent to the data acquisition and the true two-color two-photon ionization induced signal could be extracted.

The timing of the experiment was controlled by a digital delay generator (SRS DG 535). The main source of temporal jitter is given by the inaccuracy of the laser firing time. Hence, the delay of the laser was controlled by an optical feedback circuit which eliminated long-term drift. The remaining shot-to-shot jitter of about 10 ns is uncritical as far as the relative timing of primary ion pulse, sample potential switching and laser firing is concerned. It may, however, seriously deteriorate the temporal pulse widths of the measured signals, in particular if the averaging option of the transient digitizer is activated. Therefore, the whole detection system including the transient digitizer as well as the boxcar integrators recording the laser pulse energies was triggered by a fast photodiode directly detecting the excimer laser stray light.

III. RESULTS AND DISCUSSION

A. Dimers

1. Experimental data

Figure 3 shows a typical spectrum of the silver dimer and monomer signals obtained by the one-color two-photon ionization scheme using only the excitation laser. The laser wavelength was scanned in steps of 5 pm and the signals of photoionized neutral Ag_2 molecules and Ag atoms sputtered from the sample surface were recorded. At each wavelength, the measured data were obtained by the direct digitization method described above and aver-

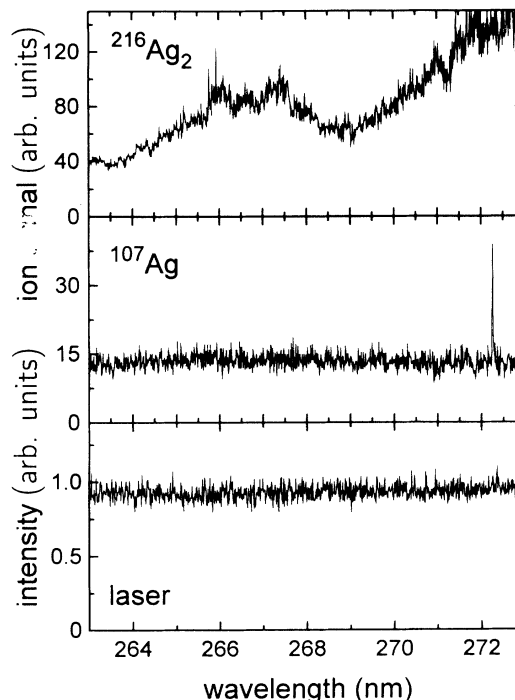


FIG. 3. One-color *R2PI* spectrum of sputtered silver dimers and atoms. (a) $^{216}\text{Ag}_2$ isotopomer; (b) ^{107}Ag isotope; (c) laser intensity variation around the nominal power density of 10^5 W/cm^2 .

aged over 1000 laser shots. In order to avoid the spectral complexity caused by isotope shifts, only the signals of the heteronuclear $^{216}\text{Ag}_2$ isotopomer and the ^{107}Ag isotope were recorded which are displayed in Figs. 3(a) and 3(b), respectively. Figure 3(c) shows the pulse energy of the ionizing laser which was kept constant at a value of $18 \mu\text{J}$ corresponding to a peak power density of approximately 10^5 W/cm^2 . As immediately seen from Fig. 3(a), the observed dimer spectra essentially exhibit a very broad feature centered around $\lambda=266 \text{ nm}$ —with some superimposed fine structure—which is due to the *X-C* transition of the Ag_2 molecule. In addition, a steeply rising signal is observed for wavelengths greater than 269 nm which is caused by resonant transitions between the ground state and the next lowest *B* state of the silver dimer. The apparent lack of well-resolved vibrational bands already indicates a high degree of internal excitation of the sputtered dimers. From the known rotational constants of the *X*, *B*, and *C* states³⁵ it is found that the *X-C* transition is almost ideally suited to study highly excited silver dimers, since in this case the equilibrium internuclear distances in the upper and lower states are virtually identical. As a consequence, the Frank-Condon parabola of this transition is extremely narrow and the interpretation of the measured spectrum (cf. Sec. III A 2) is much easier than, for instance, for the *X-B* transition. Hence, we will in the following concentrate on the *X-C* spectrum and disregard the wavelength region above 269 nm.

In contrast to the dimer spectrum, the monomer track displayed in Fig. 3 does not show any structure in the

wavelength range between 263 and 269 nm. This result is important for the following reason. During a resonant two-photon ionization process at wavelengths in this range, the total photon energy absorbed by a sputtered neutral particle amounts to approximately 9.3 eV. Hence, considering the adiabatic ionization potential of the silver dimer [7.656 eV (Ref. 36)], an excess energy of around 1.6 eV is inevitably imparted to the ionized molecule which can be rapidly converted to internal excitation. This value is quite close to the dissociation energy of the Ag_2^+ ion (1.57 eV (Ref. 35)), and, hence, significant wavelength-dependent fragmentation of the created dimer ions may be expected which would deteriorate the measured dimer spectra. Since each dissociating dimer ion must produce an Ag^+ ion, however, the resulting “fragmentation spectrum” should be reflected in the monomer ion track. From the apparent lack of any structure in Fig. 3(b), we therefore conclude that the measured dimer ionization spectra are *not* distorted by wavelength-dependent fragmentation effects.

The sharp single line observed in Fig. 3(b) at 272.27 nm is due to the autoionizing $4d^9 5s(3D)5p^2 D_{5/2}$ state of the silver atom³⁷ which is excited by single-photon absorption of Ag atoms sputtered in the metastable $4d^9 5s^2 D_{5/2}$ state.³⁸ Due to the relatively long autoionization lifetime of this state [> 70 ps (Ref. 37)], the observed width of this line (≈ 3.5 pm) essentially reflects the laser linewidth.

An important drawback of the one-color scheme is given by the fact that the cross section for the resonant transition is generally much larger than that for the ionizing step. As a consequence, in order to ionize the excited molecules with sufficient efficiency to obtain reasonable signal-to-noise ratios, one has to work with laser intensities high enough to saturate the resonant transition. To investigate the role and amount of saturation, we have taken spectra at different laser power densities. Figure 4 shows the Ag_2 spectrum obtained with a laser intensity of around 10^4 W/cm² which was the lowest possible value a meaningful spectrum could be acquired with. Due to the low signal level the data were now taken by the pulse counting method and averaged over 1000 laser shots per

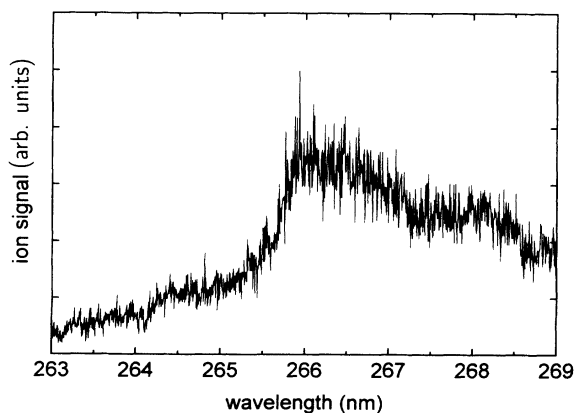


FIG. 4. One-color $R2PI$ spectrum of sputtered silver dimers. Only the signal of the $^{216}\text{Ag}_2$ isotopomer was recorded. The laser power density was kept constant around 10^4 W/cm².

point. Again, the laser intensity was kept constant within $\pm 15\%$ rms throughout the whole scan. In addition, the data were normalized to the laser power density measured at each wavelength in order to reduce the statistical noise. Comparing Figs. 3(a) and 4, it is seen that the broad features of both spectra look quite similar. In particular, no sharp structures are observed in Fig. 4 which are not already present in Fig. 3. As a consequence, one has to conclude that although the laser intensity has been reduced by roughly a factor of 10, the spectrum displayed in Fig. 4 still shows a high amount of saturation which must be accounted for in the interpretation of the data.

In principle, it is of interest to compare the spectra taken by one- and two-color resonant two-photon ionization. The basic advantage of the two-color scheme is that the intensities and wavelengths of excitation and ionization laser can be chosen independently. During our experiments with sputtered silver dimers, we have found that the (intense) ionization laser must be operated at the highest wavelength possible to still ionize the particles from the intermediate excited state, since otherwise the “nonresonant”³⁹ signal background produced by this laser becomes much larger than the resonant two-photon signal. As a consequence, we chose an ionization wavelength of $\lambda_{\text{ion}} = 400$ nm which, on the one hand, suffices to ionize all vibrational levels of the Ag_2 C state and, on the other hand, requires at least three photons to ionize all ground-state molecules except those with internal energies larger than 1.45 eV. As an example, Fig. 5 shows a dimer spectrum obtained with the excitation and ionization lasers operated at power densities of 5×10^4 and 2.5×10^6 W/cm², respectively. The data shown in the figure represent the true two-photon spectrum obtained by subtracting the signals measured with either one of the laser beams blocked from those measured with both lasers and normalizing the resulting spectrum to both laser intensities. A first observation is that due to the high power density of the ionization laser the signal levels obtained with both lasers are much higher than those measured with the excitation laser alone. It is also found that the background signal detected with only the ionization laser drops by a factor of 2 if the laser intensity is re-

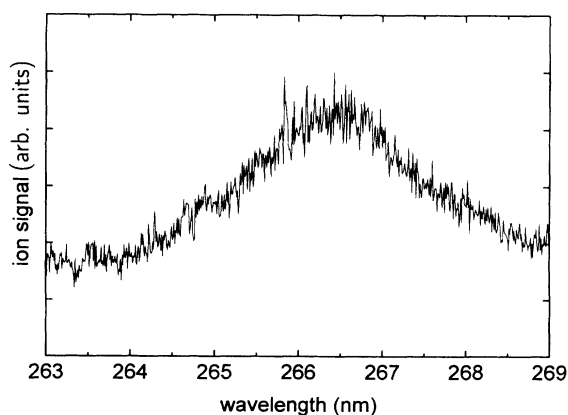


FIG. 5. Two-color $R2PI$ spectrum of sputtered silver dimers. Excitation laser: 5×10^4 W/cm²; Ionization laser: 2.6×10^6 W/cm² at $\lambda = 400$ nm.

duced by 20%. Hence, this signal depends strongly nonlinearly on the laser intensity as is expected for a non-resonant multiphoton absorption process.

If the spectrum displayed in Fig. 5 is compared to the one-color spectra of Figs. 3(a) and 4, one finds that the main structure (broad feature centered around 266 nm) is reproduced. There are, however, differences between the slopes towards both sides of the maximum, and the reliability of the spectra measured with both ionization schemes needs to be discussed. Two main points may be raised in this context. The first question concerns the background signal induced by the ionization laser. In the two-color scheme, the influence of this signal is easily eliminated from the spectrum as described above. In the one-color scheme, on the other hand, one may say that the ionization laser is scanned simultaneously with the excitation laser and can therefore contribute a wavelength-dependent nonresonant background signal which distorts the excitation spectrum. Since ionization and excitation is accomplished by the same laser, however, no difference exists between this background and the *R2PI* signal to be measured and, hence, the background cannot distort the measured spectrum. The second question concerns the possible role of continuum structure. In both ionization schemes the sum of both photon energies is scanned, and the measured spectrum may therefore, in principle, be influenced by autoionization structure of the ionization continuum. In the two-color scheme, this represents a significant problem due to the fact that the total photon energy is close to the ionization threshold. For the silver dimer, a number of autoionizing Rydberg states lying in the spectral range of interest here have recently been identified,^{35,36} the influence of which can hardly be estimated without detailed knowledge of the Frank-Condon factors for transitions between these states and the intermediate *C* state. In the one-color scheme, the total photon energy is always by at least 1.4 eV above the ionization potential of the silver dimer, and the continuum structure should play a minor role in this case. As a consequence, we feel that in the present experiments the spectra obtained with the one-color two-photon ionization scheme should be more reliable than those taken with the two-color scheme.

2. Spectrum simulation

The interpretation of the measured spectra in terms of vibrational and rotational excitation of the sputtered neutral dimers was done as follows. First, Boltzmann distributions were assumed for the population of internal states with independent vibrational and rotational tem-

peratures T_{vib} and T_{rot} , respectively. Then, measured spectra were simulated by calculating term values and two-photon ionization probabilities for all possible rovibrational transitions between the ground $X^1\Sigma_g^+$ state and the intermediate $C^1\Pi_u$ state, convoluting the resulting lines with a Gaussian of fixed width corresponding to the laser linewidth (5 pm) and sorting the resulting spectrum into wavelength slots of 5-pm width. The term values of allowed rovibrational transitions between the *X* and the *C* states were calculated by a standard Dunham expansion using the spectroscopic values of ω_e , $\omega_e x_e$, B_e , α_e , and D_e displayed in Table I. As mentioned above, it is important to include the effect of saturation into the simulation. Hence, absolute values of the transition rate

$$R_{\text{exc}} = B_{XC} \rho_{\text{exc}} \text{FCF}(v'', v') \text{HLF}(J'', J') \quad (1)$$

between rovibrational levels v'', J'' and v', J' of the *X* and *C* state, respectively, are needed. In Eq. (1), B_{XC} denotes the Einstein coefficient which may be characterized by the total oscillator strength f_{XC} of the *X-C* transition, ρ_{exc} is the spectral energy density of the excitation laser, and FCF and HLF are the Frank-Condon and Hönl-London factors of the vibrational and rotational transitions, respectively. While the HLF values were taken from Ref. 40, the Frank-Condon factors were calculated from Morse potential fits

$$V(r) = D [1 - e^{-a(r-r_e)}]^2 \quad (2)$$

to the spectroscopic constants in Table I. In more detail, the dissociation energy D of the Ag_2 *C* state was calculated from the term value T_e determined for the *X-C* transition,⁴¹ the dissociation energy of the Ag_2 ground state⁴² and the $^2S\text{-}^2P$ excitation energy of a silver atom.⁴³ Then, the constants a and r_e were calculated from ω_e , D , and B_e according to the standard formulas given in Ref. 44. It is of note that this procedure does not necessarily reproduce the experimental anharmonicity constants $\omega_e x_e$. In fact, the difference between the experimental values of $\omega_e x_e$ and the respective values calculated from the Morse potential (also displayed in Table I) may serve as a validity criterion of the Morse potential. It is seen that while the Morse formula probably represents a good approximation of the ground-state potential, the agreement is much poorer for the *C* state. As a consequence, the FCF values determined from these potentials may be erroneous for very high vibrational quantum numbers. Since no literature data are available for the second rotational constant D_e of the *C* state, we used the Kratzer relation to obtain the respective value given in Table I.

TABLE I. Spectroscopic constants of Ag_2 states and constants of Morse potentials fit to these data. All values are given in cm^{-1} unless stated otherwise. The spectroscopic data were taken from Refs. 35 and 40.

State	Spectroscopic data					Morse potential constants			
	ω_e	$\omega_e x_e$	B_e	$\alpha_e \times 10^4$	$D_e \times 10^8$	D	r_e (Å)	a (Å ⁻¹)	$\omega_e x_e$
$\text{Ag}_2 X^1\Sigma_g^+(0_g^+)$	192.4	0.643	0.048 81	2.08	1.27	134 68	2.531	1.483	0.687
$\text{Ag}_2 C^1\Pi_u(1_u)$	171.0	0.84	0.048 58	2.68	1.57	5836.4	2.534	2.000	1.25

The ionization probability P_i of a ground-state molecule with the excitation laser tuned to a resonant X - C transition was calculated from standard rate theory of two-photon ionization yielding⁴⁵

$$P_i = R_{\text{exc}} R_{\text{ion}} \frac{1}{\lambda_1 - \lambda_2} \left[\frac{e^{\lambda_1 \tau} - 1}{\lambda_1} - \frac{e^{\lambda_2 \tau} - 1}{\lambda_2} \right] \quad (3)$$

with

$$\lambda_{1,2} = \frac{2R_{\text{exc}} + R_{\text{ion}} + A_{CX}}{2} \times \left\{ 1 \pm \left[1 - \frac{4R_{\text{exc}} R_{\text{ion}}}{(2R_{\text{exc}} + R_{\text{ion}} + A_{CX})^2} \right]^{1/2} \right\}. \quad (4)$$

Here, $R_{\text{ion}} = B_{CI} \rho_{\text{ion}}$ is the ionization rate from the C state (with ρ_{ion} being the spectral energy density of the ionization laser) and A_{CX} denotes the Einstein coefficient for spontaneous C - X transitions⁴⁶ which is related to B_{XC} by the Planck-law.⁴⁷

The simulated spectra were fit to the experimental data as follows. A series of simulated spectra were calculated using the vibrational and rotational temperatures of the ground-state dimers as well as the oscillator strength of the X - C transition as parameters. First, it was found that the measured spectra can by no means be approximated if vibrational or rotational temperatures below 1000 K are assumed. Consequently, T_{vib} and T_{rot} were varied independently from each other between 1000 and 9000 K in steps of 1000 K. The values of f_{XC} were first changed between 0.1% and several 10%, but it soon turned out that the interesting region was between 1% and 10%. As a consequence, f_{XC} was then varied in this region in steps of 2.5%. The resulting set of simulated spectra was then compared to the experimental data by evaluating the sum of the squared deviations between simulated and experimental spectra. The optimal fitting parameters were found from the corresponding simulated spectrum with the least error sum. As an example, the best fit spectrum fit to the data displayed in Fig. 4 which was determined this way is displayed in Fig. 6. The resulting optimum values of T_{vib} , T_{rot} , and f_{XC} determined from fits to

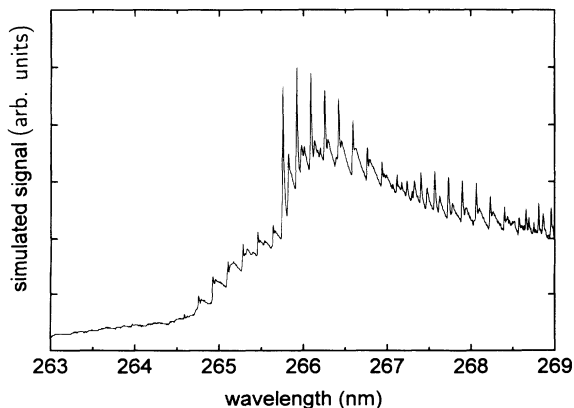


FIG. 6. Simulated $R2PI$ spectrum of silver dimers which represents the best fit to the data in Fig. 4.

several experimental spectra are displayed in Table II. First, and probably most important, all experimental data clearly reveal that the sputtered silver dimers are *hot*, i.e., are formed with internal temperatures of several thousand Kelvin. The second observation made in Table II is the striking difference between the results obtained from experimental one- and two-color spectra. While the spectra taken with the two-color ionization scheme are best approximated by T_{rot} being significantly below T_{vib} , the opposite holds for those taken with the one-color scheme. Due to the discussion given in Sec. III A 1, we believe that the one-color spectra are more reliable and, hence, conclude that the rotational temperature of sputtered silver dimers is higher than the vibrational temperature. This finding as well as the absolute temperature values given in Table II are in very good agreement with recent theoretical molecular-dynamics simulations of the dimer sputtering process which predict values of $T_{\text{vib}} = 3500$ K and $T_{\text{rot}} = 6800$ K.⁴⁸ In comparison, if the temperatures of Table II are averaged over the first three rows, we obtain mean experimental values of $T_{\text{vib}} = 2700$ K and $T_{\text{rot}} = 6700$ K. The magnitude of these temperatures matches our previous experimental finding that the threshold energy for electron-impact ionization of *sputtered* silver dimers is significantly reduced compared to that of *cold* species.⁴⁹ If converted to a temperature, the observed difference between the adiabatic ionization potential of Ag_2 [7.656 eV (Ref. 36)] and the measured appearance potential of sputtered silver dimers [7.26 eV (Ref. 50)] amounts to 4600 K. The apparent difference between vibrational and rotational population temperatures of sputtered dimers emphasizes the nonequilibrium character of the sputtering process which is due to the fast time scale (typically 10^{-13} s) on which atomic collisions leading to the sputter ejection of particles take place.

3. Discussion

Comparing our present results with available literature data on internal temperatures of sputtered diatomic molecules, we find that the temperatures determined here are of the same order as those obtained by other groups. For instance, Fayet, Wolf, and Wöste²⁶ determined vibrational temperatures of sputtered Na_2 , K_2 , and Cs_2 dimers of 1000 K and state that the rotational temperature should

TABLE II. Optimum vibrational and rotational temperatures and oscillator strengths for which the best fit to the experimental spectra was obtained. The different experimental spectra have been arbitrarily numbered and characterized by the ionization scheme employed. 1C: one-color spectra; 2C: two-color spectra.

Expt. spectrum	f_{XC} (%)	T_{vib} (K)	T_{rot} (K)
1 (1C)	7.5	3000	5000
2 (1C)	7.5	2000	8000
3 (1C)	2.5	3000	7000
1 (2C)	5	8000	4000
2 (2C)	2.5	8000	4000

be of the same magnitude. De Jonge and co-workers measured the internal population distribution of S_2 dimers sputtered either from elementary sulphur or CS_2 targets^{24,25} and found quasithermal vibrational population distributions showing a vibrational temperature of 1500 K, whereas the rotational population was found to be strongly nonthermal. Most recent investigations of sputtered MgO molecules carried out by Fournier *et al.*⁵¹ reveal vibrational and rotational temperatures of 5000 and 1750 K, respectively. It should be noted, however, that the systems studied in Refs. 24–26, and 51 represent rather special cases in view of the sputtering processes involved. The alkali metal targets investigated in Ref. 26, for instance, have very low melting temperatures and, hence, atomic ejection processes induced by ion bombardment are not necessarily dominated by (fast) collisional mechanisms. In contrast, it is very likely that at least part of the ejected species are emitted by thermal processes. The sulphur dimers studied in Refs. 24 and 25, on the other hand, represent a typical case of a strongly bound molecule which, as a whole, is only very weakly bound to the surface. These molecules can be very efficiently sputtered by the so-called *single collision* or *direct emission* mechanism, where the molecule pre-existing at the surface is knocked off by a single collision from underneath. The same mechanism has also been proposed to be responsible for the formation of sputtered metal oxide molecules³ like those studied in Ref. 51. It has been shown that in this case the vibrational and rotational excitation of the ejected molecule will be anticorrelated depending on the original orientation of the molecule at the surface^{4,52} and hence, the combination of high vibrational and low rotational excitation can be rationalized. The situation is different for sputtered metal dimers, since here no pre-formed molecules exist at the surface. Since the surface binding energy of the individual atoms is of the same order as the bond strength of the dimer, the single collision mechanism does not work in this case and the two atoms must be ejected rather independently from each other. It is easily understandable that this emission process will in general lead to a substantial rotational and vibrational excitation of the sputtered dimer.

B. Larger clusters

In view of the high internal temperatures of sputtered molecules obtained in the preceding section and the enormously complex spectra even of cold metal trimers,⁵³ it is clear that resonant multiphoton ionization spectroscopy is not appropriate to investigate the internal energy of sputtered clusters larger than diatomic molecules. A promising technique, however, is in this case given by the single photon ionization mechanism, provided the photon energy is close enough to the ionization threshold to prevent substantial fragmentation upon ionization. We have recently shown that sputtered silver clusters up to Ag_{20} can be efficiently detected by this method if the ionization is performed by an excimer laser operated at a photon energy of 6.4 eV ($\lambda = 193$ nm), since most of the silver clusters have ionization potentials around or slight-

ly below this energy.⁵⁴ An important exception, however, is given by the Ag_6 cluster. The ionization potential of this cluster was measured in Ref. 54 to be as large as 7.15 eV. As a consequence, Ag_6 clusters are *not* detectable at a wavelength of 193 nm in a supersonic silver cluster beam.⁵⁵ If the laser wavelength is changed to 157 nm corresponding to a photon energy of 7.9 eV, the cold cluster *is* detected⁵⁵ since now the photon energy is above the ionization threshold. In contrast, large Ag_6 signals are found in our experiments at *both* laser wavelengths. Figure 7 shows part of the mass spectrum of sputtered neutral silver clusters obtained with the excimer laser operated at 193 and 157 nm, respectively. Both spectra were taken with comparable pulse energies of 0.5 mJ corresponding to a laser power density of several 10^5 W/cm². As seen from the figure, the signals of Ag_5 and Ag_7 are comparable for both wavelengths since for these clusters both photon energies are above the respective ionization potentials [6.35 and 6.4 eV (Ref. 54)]. The signal measured for Ag_6 , on the other hand, is by a factor of 2 lower if the longer wavelength photons are used to ionize the cluster. It is of note that the dependence of all signals on the laser intensity is strictly linear in the region of low laser power density. In particular, no significant change of the spectra displayed in Fig. 7 besides an overall reduction of intensities is observed if the laser power density is decreased by as much as two orders of magnitude. We take this as an indication that the contribution of fragmentation of larger clusters to the measured signals is small and, hence, in both cases the Ag_6 signal is generated by a single photon ionization process. This finding is of particular importance since then at $\lambda = 193$ nm *only* those Ag_6 clusters are ionized which possess an internal energy of at least 0.75 eV. At 157 nm, on

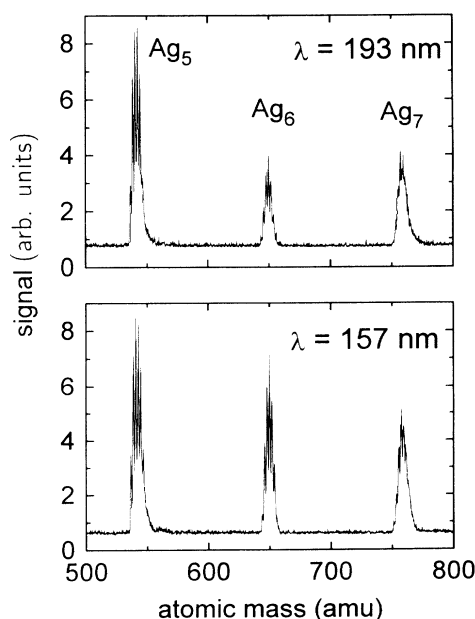


FIG. 7. Mass spectra of sputtered neutral silver clusters taken by single-photon ionization at two different wavelengths of the ionizing laser.

the other hand, we detect all Ag_6 clusters present in the ionization volume regardless of their internal energy. From these experiments, we therefore conclude that around 50% of the sputtered neutral Ag_6 clusters contain internal energies in excess of 0.75 eV.

Looking through the literature, one finds that virtually no data of this kind have been published to date. There are, however, numerous papers investigating the unimolecular decomposition of sputtered cluster ions.^{28–33} These studies provide evidence that an abundant number of sputtered clusters leave the surface in excited rovibrational states with internal energies above the cluster's dissociation threshold. These clusters will eventually decompose during their passage away from the surface, until at large distances mainly the stable end products of such fragmentation chains are detected experimentally. From fragmentation studies, little information can be gained about the *stable* clusters which contain internal energies below the dissociation threshold. Therefore, to our knowledge the present data represent the first direct experimental hint on the quantitative amount of internal energy stored in sputtered clusters larger than dimers.

IV. CONCLUSIONS

Using resonant two-photon ionization spectroscopy, we have shown that sputtered silver dimers are formed in highly excited internal states. In particular, vibrational

and rotational temperatures of 2000–3000 K and 5000–8000 K were determined by simulation of the measured spectra. These results agree very well with corresponding theoretical predictions obtained from recent molecular dynamics simulations of the molecule sputtering process.

Sputtered silver clusters larger than dimers are practically undetectable by multiphoton ionization techniques. They can, however, be detected very efficiently if single-photon ionization from a uv laser is used. From the comparison of cluster mass spectra taken at different laser wavelengths, it is concluded that, for instance, around 50% of the sputtered silver hexamers contain internal energies above 0.75 eV. A more detailed study of the internal energy distribution would be possible if the ionizing laser wavelength could be continuously tuned over the ionization threshold of the sputtered clusters. This, however, requires tunable vuv radiation in the wavelength range around 150 nm which is presently not available in our lab.

ACKNOWLEDGMENTS

The author is greatly indebted to H. Oechsner for his continuous and stimulating support. We would like to express our gratitude to W. Demröder and V. Beutel for an introduction into the field of laser spectroscopy and numerous discussions. Thanks are also due to the Deutsche Forschungsgemeinschaft for financial support in the frame of the Sonderforschungsbereich 91.

¹For a detailed description, see R. Behrisch, in *Sputtering by Particle Bombardment*, edited by R. Behrisch and K. Wittmaack (Springer, Berlin, 1991), Vol. III, p. 3.

²A. Benninghoven, *Surf. Sci.* **35**, 427 (1973).

³H. Oechsner, H. Schoof, and E. Stumpe, *Surf. Sci.* **76**, 343 (1978).

⁴P. Sigmund, H. M. Urbassek, and D. Matagrano, *Nucl. Instrum. Methods B* **14**, 495 (1986).

⁵G. P. Können, A. Tip, and A. E. de Vries, *Radiat. Eff.* **21**, 269 (1974).

⁶R. Hoogerbrugge and P. G. Kistemaker, *Nucl. Instrum. Methods B* **21**, 37 (1987).

⁷W. Gerhard, *Z. Phys. B* **22**, 31 (1975).

⁸K. J. Snowdon, R. Hentschke, W. Heiland, and P. Hertel, *Z. Phys. A* **318**, 261 (1984).

⁹D. E. Harrison, Jr. and C. B. Delaplain, *J. Appl. Phys.* **47**, 2252 (1976).

¹⁰N. Winograd, D. E. Harrison, Jr., and B. J. Garrison, *Surf. Sci.* **78**, 467 (1978).

¹¹B. J. Garrison, N. Winograd, and D. E. Harrison, Jr., *J. Chem. Phys.* **69**, 1440 (1978).

¹²B. J. Garrison, N. Winograd, and D. E. Harrison, Jr., *Phys. Rev. B* **18**, 6000 (1978).

¹³N. Winograd, K. E. Foley, B. J. Garrison, and D. E. Harrison, Jr., *Phys. Lett. A* **73**, 253 (1979).

¹⁴N. Winograd, B. J. Garrison, T. Fleisch, W. N. Delgass, and D. E. Harrison, Jr., *J. Vac. Sci. Technol.* **16**, 629 (1979).

¹⁵S. P. Holland, B. J. Garrison, and N. Winograd, *Phys. Rev.*

Lett. **44**, 756 (1980).

¹⁶B. J. Garrison, *J. Am. Chem. Soc.* **102**, 6553 (1980).

¹⁷N. Winograd, B. J. Garrison, and D. E. Harrison, Jr., *J. Chem. Phys.* **73**, 3473 (1980).

¹⁸D. E. Harrison, Jr., P. Avouris, and R. Walkup, *Nucl. Instrum. Methods B* **18**, 321 (1987).

¹⁹A. Wucher and B. J. Garrison, *Surf. Sci.* **260**, 257 (1992).

²⁰A. Wucher and B. J. Garrison, *Phys. Rev. B* **46**, 4855 (1992).

²¹K. J. Snowdon and W. Heiland, *Z. Phys. A* **318**, 275 (1984).

²²C. M. Loxton, I. S. T. Tsong, and D. A. Reed, *Nucl. Instrum. Methods B* **2**, 465 (1984).

²³E. W. Thomas and L. Efstathiou, *Nucl. Instrum. Methods B* **2**, 479 (1984).

²⁴R. de Jonge, T. Baller, M. G. Tenner, A. E. de Vries, and K. J. Snowdon, *Europhys. Lett.* **2**, 499 (1986); *Nucl. Instrum. Methods B* **17**, 213 (1986).

²⁵R. de Jonge, K. W. Benoist, J. W. F. Majoor, and A. E. de Vries, *Nucl. Instrum. Methods B* **28**, 214 (1987).

²⁶P. Fayet, J. P. Wolf, and L. Wöste, *Phys. Rev. B* **33**, 6792 (1986).

²⁷P. Sigmund, in *Sputtering by Particle Bombardment*, edited by R. Behrisch (Springer, Berlin, 1981), Vol. I, pp. 10 and 15.

²⁸N. K. Dzhemilev and S. V. Verkhoturov, *Izv. Akad. Nauk SSSR, Ser. Fiz.* **49**, 1831 (1985).

²⁹N. K. Dzhemilev, U. K. Rasulev, and S. V. Verkhoturov, *Nucl. Instrum. Methods B* **29**, 531 (1987).

³⁰N. K. Dzhemilev, S. V. Verkhoturov, and I. V. Veriovin, *Nucl. Instrum. Methods B* **51**, 219 (1990).

- ³¹N. K. Dzhemilev, A. M. Goldenberg, I. V. Veriovkin, and S. V. Verkhoturov, *Int. J. Mass. Spectrom. Ion. Proc.* **107**, R19 (1991).
- ³²W. Begemann, S. Dreihöfer, K. H. Meiwes-Broer, and H. O. Lutz, *Z. Phys. D* **3**, 183 (1986).
- ³³W. Begemann, K. H. Meiwes-Broer, and H. O. Lutz, *Phys. Rev. Lett.* **56**, 2248 (1986).
- ³⁴A. Wucher, M. Wahl, and H. Oechsner, *Nucl. Instrum. Methods B* **82**, 337 (1993).
- ³⁵V. Beutel, H.-G. Krämer, G. L. Bhale, M. Kuhn, K. Weyers, and W. Demtröder, *J. Chem. Phys.* **98**, 2699 (1993).
- ³⁶V. Beutel, G. L. Bhale, M. Kuhn, and W. Demtröder, *Chem. Phys. Lett.* **185**, 313 (1991).
- ³⁷S. Baier, M. Martins, B. R. Müller, M. Schulze, and P. Zimmermann, *J. Phys. B* **23**, 3095 (1990).
- ³⁸A. Wucher, W. Berthold, H. Oechsner, and K. Franzreb (unpublished).
- ³⁹Due to the fact that almost all ground-state rovibrational levels of sputtered molecules are populated, any chosen laser wavelength will find at least a near resonance and, hence, the term *nonresonant* may be somewhat misleading in this case.
- ⁴⁰G. Herzberg, *Molecular Spectra and Molecular Structure, Vol. I: Spectra of Diatomic Molecules* (Van Nostrand Reinhold, New York, 1950), p. 208. [The formulas given in the reference were divided by $(2J+1)/2$ to obtain the HLF used here.]
- ⁴¹C. M. Brown and M. L. Ginter, *J. Mol. Spectrosc.* **69**, 25 (1978).
- ⁴²M. D. Morse, *Chem. Rev.* **86**, 1049 (1986).
- ⁴³C. E. Moore, *Atomic Energy Levels*, Natl. Bur. Stand. Ref. Data Ser., Natl. Bur. Stand. (U.S.) Circ. No. 35 (NBS, Washington, 1971), Vol. III, pp. 48ff.
- ⁴⁴*Molecular Spectra and Molecular Structure, Vol. I: Spectra of Diatomic Molecules* (Ref. 39), p. 101.
- ⁴⁵J. P. Reilley and K. L. Kompa, *J. Chem. Phys.* **73**, 5468 (1980).
- ⁴⁶Spontaneous transitions to other even states below the C state (except the ground state) are neglected due to the λ^{-3} dependence of the emission coefficient.
- ⁴⁷W. Demtröder, *Laser Spectroscopy* (Springer, Berlin, 1991), p. 12.
- ⁴⁸A. Wucher and B. J. Garrison, *Nucl. Instrum. Methods B* **82**, 352 (1993).
- ⁴⁹K. Franzreb, A. Wucher, and H. Oechsner, *Surf. Sci. Lett.* **279**, L225 (1992).
- ⁵⁰K. Franzreb, A. Wucher, and H. Oechsner, *Z. Phys. D* **17**, 51 (1990).
- ⁵¹P. G. Fournier, J. Fournier, B. Bellaoui, O. Benoist d'Azy, and G. Taieb, *Nucl. Instrum. Methods B* **78**, 144 (1993).
- ⁵²H. M. Urbassek, *J. Phys. B* **20**, 3105 (1987).
- ⁵³V. Beutel, H.-J. Böhm, W. Demtröder, H.-A. Eckel, J. Gress, M. Kuhn, and A. Sasso, *Laser Chem.* **11**, 209 (1991).
- ⁵⁴C. Jackschath, I. Rabin, and W. Schulze, *Z. Phys. D* **22**, 517 (1992).
- ⁵⁵K. LaiHing, P. Y. Cheng, and M. A. Duncan, *Z. Phys. D* **13**, 161 (1989).

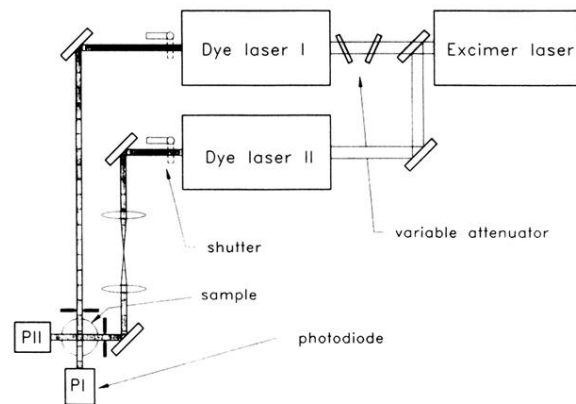


FIG. 2. Optical setup for resonant two-photon ionization and single-photon ionization of sputtered clusters.